



Vertical Split Rim: Causes and Prevention



NOTICE

This document is disseminated under the sponsorship of the Department of Transportation in the interest of information exchange. The United States Government assumes no liability for its contents or use thereof. Any opinions, findings and conclusions, or recommendations expressed in this material do not necessarily reflect the views or policies of the United States Government, nor does mention of trade names, commercial products, or organizations imply endorsement by the United States Government. The United States Government assumes no liability for the content or use of the material contained in this document.

NOTICE

The United States Government does not endorse products or manufacturers. Trade or manufacturers' names appear herein solely because they are considered essential to the objective of this report.

REPORT DOCUMENTATION PAGE			Form Approved OMB No. 0704-0188	
Public reporting burden for this collection of information is estimated to average 1 hour per response, including the time for reviewing instructions, searching existing data sources, gathering, and maintaining the data needed, and completing and reviewing the collection of information. Send comments regarding this burden estimate or any other aspect of this collection of information, including suggestions for reducing this burden, to Washington Headquarters Services, Directorate for Information Operations and Reports, 1215 Jefferson Davis Highway, Suite 1204, Arlington, VA 22202-4302, and to the Office of Management and Budget, Paperwork Reduction Project (0704-0188), Washington, DC 20503.				
1. AGENCY USE ONLY (Leave blank)		2. REPORT DATE September 2023		3. REPORT TYPE AND DATES COVERED Technical Report
4. TITLE AND SUBTITLE Vertical Split Rim: Causes and Prevention			5. FUNDING NUMBERS DTFR53-11-D-00008 Task Order 334	
6. AUTHOR(S) Kerry Jones – ORCID 0000-0001-9414-1872 Scott Cummings – ORCID 0009-0006-6490-3171 Harry Tournay (Retired)				
7. PERFORMING ORGANIZATION NAME(S) AND ADDRESS(ES) Transportation Technology Center, Inc. 55500 DOT Road Pueblo, CO 81001			8. PERFORMING ORGANIZATION REPORT NUMBER	
9. SPONSORING/MONITORING AGENCY NAME(S) AND ADDRESS(ES) U.S. Department of Transportation Federal Railroad Administration Office of Railroad Policy and Development Office of Research, Development and Technology Washington, DC 20590			10. SPONSORING/MONITORING AGENCY REPORT NUMBER DOT/FRA/ORD-23/30	
11. SUPPLEMENTARY NOTES COR: Monique Ferguson Stewart (John Punwani)				
12a. DISTRIBUTION/AVAILABILITY STATEMENT This document is available to the public through the FRA website .			12b. DISTRIBUTION CODE	
13. ABSTRACT (Maximum 200 words) Vertical split rim (VSR) is a serious railway wheel failure mode that requires further research. Visual clues are not usually present until the crack propagates through the rim. To better understand the root causes of VSRs, the Federal Railroad Administration (FRA) and the Association of American Railroads (AAR) have jointly funded the investigation of this problem. To better understand VSR, Transportation Technology Center, Inc. (TTCI) attempted to create this defect in a laboratory. A deep slit was cut into the tread of the wheel. After 1.8 million cycles at loads of 36–50 kips, the crack still did not propagate and no VSR was created. This test followed previous attempts of higher vertical wheel loads, but without a cut, that did not create VSR. Wheel manufacturers and TTCI previously tried to create a VSR under controlled conditions using a rolling load machine. In both previous instances, a VSR was not created.				
14. SUBJECT TERMS Vertical split rim, VSR, wheel cracks, finite element analysis, FEA, residual stress, fatigue damage models, finite element, FE			15. NUMBER OF PAGES 29	
			16. PRICE CODE	
17. SECURITY CLASSIFICATION OF REPORT Unclassified	18. SECURITY CLASSIFICATION OF THIS PAGE Unclassified	19. SECURITY CLASSIFICATION OF ABSTRACT Unclassified	20. LIMITATION OF ABSTRACT	

NSN 7540-01-280-5500

Standard Form 298 (Rev. 2-89)
Prescribed by ANSI Std. Z39-18
298-102

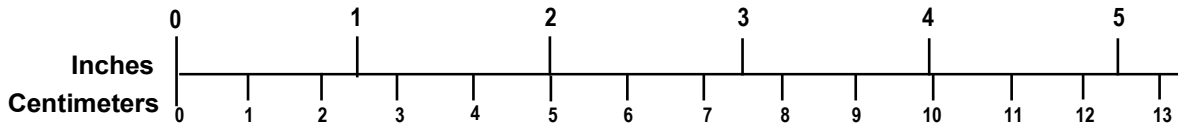
METRIC/ENGLISH CONVERSION FACTORS

ENGLISH TO METRIC

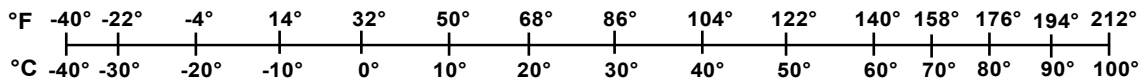
METRIC TO ENGLISH

<p>LENGTH (APPROXIMATE)</p> <p>1 inch (in) = 2.5 centimeters (cm)</p> <p>1 foot (ft) = 30 centimeters (cm)</p> <p>1 yard (yd) = 0.9 meter (m)</p> <p>1 mile (mi) = 1.6 kilometers (km)</p>	<p>LENGTH (APPROXIMATE)</p> <p>1 millimeter (mm) = 0.04 inch (in)</p> <p>1 centimeter (cm) = 0.4 inch (in)</p> <p>1 meter (m) = 3.3 feet (ft)</p> <p>1 meter (m) = 1.1 yards (yd)</p> <p>1 kilometer (km) = 0.6 mile (mi)</p>
<p>AREA (APPROXIMATE)</p> <p>1 square inch (sq in, in²) = 6.5 square centimeters (cm²)</p> <p>1 square foot (sq ft, ft²) = 0.09 square meter (m²)</p> <p>1 square yard (sq yd, yd²) = 0.8 square meter (m²)</p> <p>1 square mile (sq mi, mi²) = 2.6 square kilometers (km²)</p> <p>1 acre = 0.4 hectare (he) = 4,000 square meters (m²)</p>	<p>AREA (APPROXIMATE)</p> <p>1 square centimeter (cm²) = 0.16 square inch (sq in, in²)</p> <p>1 square meter (m²) = 1.2 square yards (sq yd, yd²)</p> <p>1 square kilometer (km²) = 0.4 square mile (sq mi, mi²)</p> <p>10,000 square meters (m²) = 1 hectare (ha) = 2.5 acres</p>
<p>MASS - WEIGHT (APPROXIMATE)</p> <p>1 ounce (oz) = 28 grams (gm)</p> <p>1 pound (lb) = 0.45 kilogram (kg)</p> <p>1 short ton = 2,000 pounds (lb) = 0.9 tonne (t)</p>	<p>MASS - WEIGHT (APPROXIMATE)</p> <p>1 gram (gm) = 0.036 ounce (oz)</p> <p>1 kilogram (kg) = 2.2 pounds (lb)</p> <p>1 tonne (t) = 1,000 kilograms (kg) = 1.1 short tons</p>
<p>VOLUME (APPROXIMATE)</p> <p>1 teaspoon (tsp) = 5 milliliters (ml)</p> <p>1 tablespoon (tbsp) = 15 milliliters (ml)</p> <p>1 fluid ounce (fl oz) = 30 milliliters (ml)</p> <p>1 cup (c) = 0.24 liter (l)</p> <p>1 pint (pt) = 0.47 liter (l)</p> <p>1 quart (qt) = 0.96 liter (l)</p> <p>1 gallon (gal) = 3.8 liters (l)</p> <p>1 cubic foot (cu ft, ft³) = 0.03 cubic meter (m³)</p> <p>1 cubic yard (cu yd, yd³) = 0.76 cubic meter (m³)</p>	<p>VOLUME (APPROXIMATE)</p> <p>1 milliliter (ml) = 0.03 fluid ounce (fl oz)</p> <p>1 liter (l) = 2.1 pints (pt)</p> <p>1 liter (l) = 1.06 quarts (qt)</p> <p>1 liter (l) = 0.26 gallon (gal)</p> <p>1 cubic meter (m³) = 36 cubic feet (cu ft, ft³)</p> <p>1 cubic meter (m³) = 1.3 cubic yards (cu yd, yd³)</p>
<p>TEMPERATURE (EXACT)</p> <p>$[(x-32)(5/9)] \text{ } ^\circ\text{F} = y \text{ } ^\circ\text{C}$</p>	<p>TEMPERATURE (EXACT)</p> <p>$[(9/5) y + 32] \text{ } ^\circ\text{C} = x \text{ } ^\circ\text{F}$</p>

QUICK INCH - CENTIMETER LENGTH CONVERSION



QUICK FAHRENHEIT - CELSIUS TEMPERATURE CONVERSION



For more exact and or other conversion factors, see NIST Miscellaneous Publication 286, Units of Weights and Measures. Price \$2.50 SD Catalog No. C13 10286

Updated 6/17/98

Contents

Executive Summary	1
1. Introduction	2
1.1 Background	2
1.2 Objectives	3
1.3 Overall Approach	3
1.4 Scope	4
1.5 Organization of the Report	4
2. VSR Rates in Freight Cars and Locomotives.....	5
2.1 Background and Method	5
2.2 Findings	5
3. Residual Stresses in New Wheels.....	7
3.1 Background	7
3.2 Test Method.....	8
3.3 Results	8
4. Wheel-Rail Rolling Contact Stress and Fatigue Analysis.....	10
4.1 Stress Analysis Method and Parameters	10
4.2 Stress Analysis Results.....	12
4.3 Findley Fatigue Model Background, Method, and Parameters.....	14
4.4 Findley Fatigue Model Results.....	14
4.5 Strain-Based Critical Plane Fatemi-Socie Fatigue Model Background, Method, and Parameters	15
4.6 Strain-Based Critical Plane Fatemi-Socie Fatigue Model Results.....	16
4.7 Stress and Fatigue Analysis Findings.....	18
5. Laboratory Creation of a VSR.....	20
5.1 Background	20
5.2 Test Method.....	20
5.3 Results	21
6. Conclusions	23
7. References	24

Illustrations

Figure 1. VSR Wheel.....	2
Figure 2. Shattered Rim Wheel.....	3
Figure 3. Broken Rims and Flanges per Million Miles in Locomotive Wheels.....	5
Figure 4. Broken Rims and Flanges per Million Miles in Freight Car Wheels.....	6
Figure 5. Wheel with Residual Stress Sample Removed.....	7
Figure 6. Residual Stress Sample, with EDM Slit Indicated in Red.....	7
Figure 7. Axial Residual Stress from Tread Surface to Depth of 1.60 inches.....	9
Figure 8. Axial Residual Stress in the Near Surface Region.....	9
Figure 9. FE Model: (left) Boundary Conditions, (right) Wheel-Rail Contact Interface.....	10
Figure 10. Cross Section of Refined Meshes for Rail and Wheel.....	11
Figure 11. Refined Meshes and Contact Areas for Rail and Wheel.....	11
Figure 12. Stress and Fatigue Index Measurement Locations in the Wheel.....	12
Figure 13. Cyclic Residual Stress Evolution in the Wheel [5].....	12
Figure 14. Residual Stress Distribution after the Fifth Load Cycle Along a Line in the Wheel's Cross Section of Interest [7].....	13
Figure 15. Residual Strain Distribution after the Fifth Load Cycle Along a Line in the Wheel's Cross Section of Interest [7].....	13
Figure 16. Maximum Findley Fatigue Index for $\kappa = 0$ [7].....	14
Figure 17. Maximum Findley Fatigue Index for $\kappa = 0.3$ [7].....	15
Figure 18. Maximum Findley Fatigue Index for $\kappa = 1$ [7].....	15
Figure 19. Physical Basis of the Fatemi-Socie Fatigue Model [9].....	16
Figure 20. Maximum Fatemi-Socie Fatigue Index for $\eta = 0$	17
Figure 21. Maximum Fatemi-Socie Fatigue Index for $\eta = 1$	17
Figure 22. Maximum Fatemi-Socie Fatigue Index for $\eta = 3$	18
Figure 23. Maximum Fatemi-Socie Fatigue Index for $\eta = 5$	18
Figure 24. Rolling Load Machine at the TTC.....	20
Figure 25. Geometry of Slit in Wheel.....	21
Figure 26. Rolling Load Cycle Count.....	21

Executive Summary

The Federal Railroad Administration (FRA) and the Association of American Railroads (AAR) jointly funded the investigation of vertical split rims (VSR) related to broken wheel rims, which is one of the leading causes of FRA reportable wheel-related accidents. In such instances, visual clues are not usually present until a crack in the wheel propagates through the rim.

The team focused on four areas of emphasis for this research: 1) an analysis of VSR rates in freight cars and locomotives; 2) measurement of residual stresses in new wheels; 3) a Finite Element Analysis (FEA) of stresses due to flaws of varying shapes, orientation, and location; and 4) creation of a VSR in the laboratory.

Researchers found that the analysis suggests locomotives have a lower VSR failure rate than cars by a factor of 2,470, based on failures per service mile. The team did not research the source of this difference, as it was not within the scope of the current project; however, the team suspects that differences in the operating and maintenance environments between the two types of wheels are likely contributors.

The axial residual stress was measured in new, as-manufactured wheels from two different suppliers. Results showed a strong residual compressive stress field near the surface, rising to slightly tensile stress as the measurements progressed along the wheel radius, then tapering to near neutral stress deeper in the wheels. The yielding of the tread surface layer that occurs naturally during the work hardening process produces a modified residual stress pattern. Previous work at the Facility for Accelerated Service Testing (FAST) using FEA indicate the wheels work harden quickly in service, possibly minimizing the influence of minor variations in the as-manufactured residual stress profile developed during the heat treatment and quenching operations.

Researchers performed FEA of residual stresses and fatigue that developed in a railroad wheel at the Center for Railway Research at Texas A&M University. The predicted steady-state axial residual tensile stresses agreed well with reported values in both magnitude and radial depth. These stress-strain responses were then used for two different fatigue criteria, the Findley model and the Fatemi-Socie model. These two fatigue damage models agreed that the critical radial depth for fatigue initiation in wheels is 0.15 inches considering both contact stress and residual stress. The median radial depth of VSR crack origins from failed wheels has been reported at 0.17 inches, thus the analysis is considered accurate in this prediction.

Laboratory creation of a VSR was attempted in this research to determine parameters under which VSRs form. The test consisted of cutting a deep slit into the tread of a service worn wheel, then placing the wheel on a rolling load machine under various vertical loads and ultrasonically monitoring the crack growth. The applied load began at 36 kips and finished at 50 kips. After 1.8 million cycles, the crack did not propagate. Previous attempts using higher vertical wheel loads but without a cut also failed to create a VSR. Wheel manufacturers and the research team previously attempted to create a VSR under controlled conditions using a rolling load machine. A VSR was not created in either previous attempt.

1. Introduction

Broken wheel rims are the leading cause of reported wheel-related accidents, and vertical split rims (VSR) are an increasingly large component of the broken rim problem. In this joint project by the Federal Railroad Administration (FRA) and the Association of American Railroads (AAR), the research team found that a visual inspection of wheel damage cannot detect a wheel in the early stages of a VSR failure because the cracks propagate vertically under the tread surface. Ultrasonic testing can be used to detect the near-surface delamination that is not uncommon in service worn wheels and is essentially found on all VSR failed wheels.

1.1 Background

FRA and AAR have previously funded research on VSRs that included inspection and analysis of VSR wheels, residual stress evaluation, micro-cleanliness testing, and load cycling of wheels with preexisting horizontal cracks [1]. To date, the root cause of the VSR failure mode has not been found. VSR wheels usually have shells or spalls on the tread surface near the VSR and horizontal cracking or delamination at a depth of approximately 0.25 inch below the tread surface. VSRs tend to occur more frequently in the winter as compared to the summer. This may be due in part to an increase in wheel shelling in the winter. Axial residual stresses may play a role in VSR crack propagation once the crack has reached a depth of approximately 0.50 inch below the tread surface.

Transportation Technology Center, Inc. (TTCI), Griffin Wheel Company, and Standard Steel co-funded parametric finite element analysis (FEA) modeling of VSR wheels before the measurement of wheel axial residual stresses was made [1]. Therefore, the residual stresses are larger in service worn wheels than the residual stresses accounted for in the model, which may influence the results. Past FEA modeling of VSR wheels has been limited to subsurface defects and excluded defects that break the tread surface.

VSR and shattered rims are the main failure modes for broken wheel rim accidents. [Figure 1](#) and [Figure 2](#) show examples of VSR and shattered rim wheels.



Figure 1. VSR Wheel



Figure 2. Shattered Rim Wheel

1.2 Objectives

The team focused on four areas of emphasis for this research: 1) determine the rate of reported VSRs in freight car and locomotive wheels; 2) compare residual stresses in new, as-manufactured wheels; 3) perform FEA of a wheel rolling on a rail to assess the subsurface fatigue environment associated with rolling contact in the presence of residual stresses developed from cold working; and 4) create several VSRs in the laboratory and find parameters that lead to delamination and VSRs.

1.3 Overall Approach

For each of the main tasks in this research, the following quantitative methods were used.

- VSR data were extracted from FRA's Accident Database [2]
- Eight new, as-manufactured, wheels were sampled for residual stresses
- Researchers contracted with Texas A&M University's Center for Railway Research to determine stress and fatigue effects that occur during service. The states of stress and strain that occur during rolling contact are quite complex and an awareness of the effects is critical to correctly modeling the residual stresses and fatigue that develop under rolling contact.
- The attempt to create a VSR in the laboratory was performed quantitatively. Load and cycle data were recorded, but the crack did not propagate.

1.4 Scope

The scope of this research was limited to VSR defects, residual stresses in new wheels, and the fatigue properties of wheels.

1.5 Organization of the Report

[Section 2](#) presents existing VSR rates in freight cars and locomotives. [Section 3](#) discusses the residual stresses in new wheels. [Section 4](#) describes the FEA modeling of stress field and fatigue. [Section 5](#) details the VSR laboratory creation attempt. Conclusions and a summation of the work performed are found in [Section 6](#).

2. VSR Rates in Freight Cars and Locomotives

2.1 Background and Method

The research team investigated the historical frequency of VSRs in freight cars and locomotives using FRA's Office of Safety Analysis database on accident causes [2]. This public database contains accident information for the United States from 1975 to present. There is no code for VSR, but defect codes E60C, E60L, E61C, and E61L were recorded for freight car broken flanges, locomotive broken flanges, freight car broken rims, and locomotive broken rims, respectively. The team gathered the number of locomotives and freight cars in service for each year from AAR [2].

2.2 Findings

Between 1995 and 2012, seven accidents were attributed to locomotive wheels with broken flanges or broken rims. During the same time, 297 accidents were attributed to freight car broken flanges or broken rims. To normalize the data, the locomotive numbers were divided by the number of freight road service miles [3]. [Figure 3](#) shows the frequency of broken rims and flanges in locomotives. The freight car broken rims and flanges were divided by the total freight car miles and these data are plotted in [Figure 4](#).

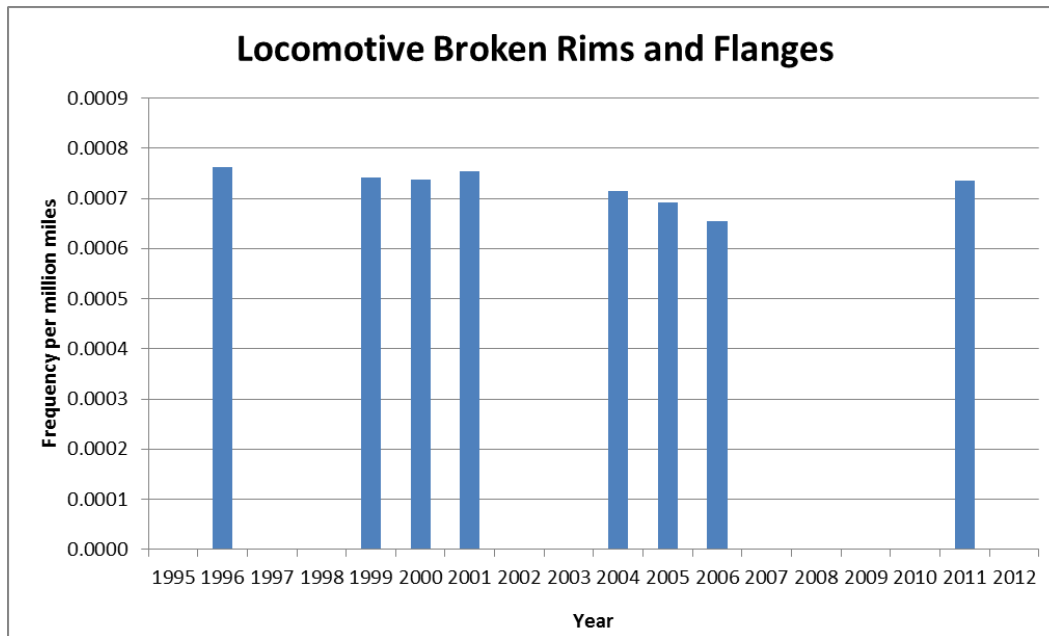


Figure 3. Broken Rims and Flanges per Million Miles in Locomotive Wheels

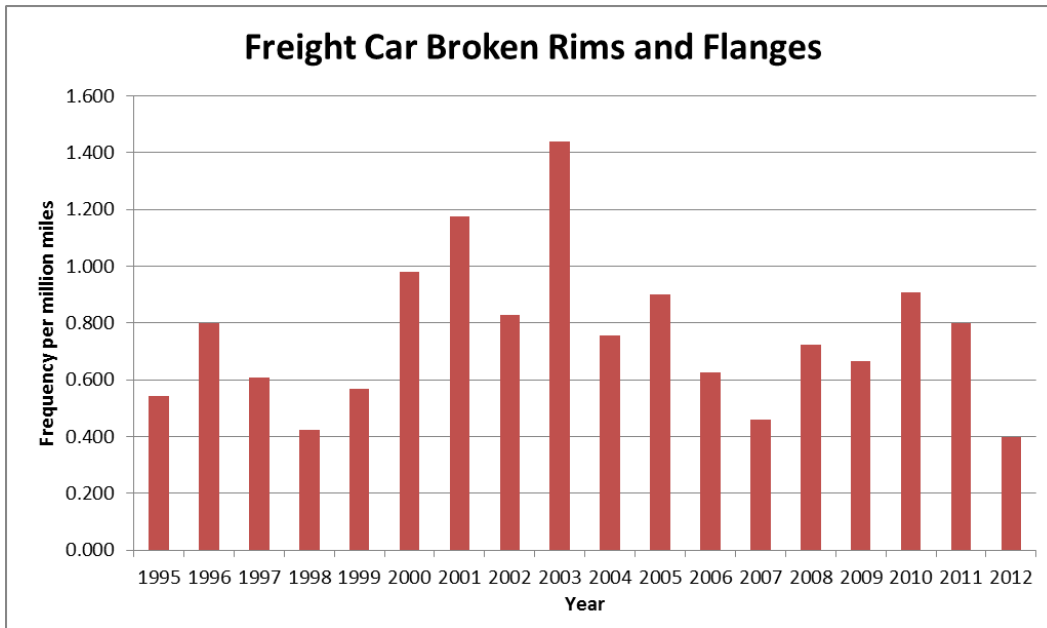


Figure 4. Broken Rims and Flanges per Million Miles in Freight Car Wheels

From 1995 to 2012, the overall frequency of broken rims and flanges for locomotive wheels was 0.0003 per million miles; for freight cars, the frequency was 0.741 per million miles.

Investigating the source of this VSR difference between locomotive wheels and freight car wheels is not within the scope of this research. However, the operating and maintenance environments between the two types of wheels may provide clues about potential sources of this difference (e.g., locomotive wheels are rarely exposed to the same tread braking demands as freight car wheels, and are not exposed to high temperatures).

Preliminary work shows that the temperatures experienced by freight car wheels during tread braking may temporarily produce a residual stress environment in the wheel rim that is more conducive to VSR crack propagation [5]. Second, the maintenance of locomotive wheels is managed differently than freight car wheels. Locomotive wheels are reprofiled more frequently to maximize the total asset life, and small tread shells are removed from locomotive wheels as they are reprofiled. Freight car wheels are allowed to remain in service until reaching industry-condemning limits, and thus have more opportunity to accumulate service miles with small tread shells and small shallow rim cracks.

3. Residual Stresses in New Wheels

3.1 Background

The axial residual stress in a wheel can be measured even after it is sectioned. There are two primary methods to determine the residual stress for a wheel section: the slitting method and the x-ray diffraction method. For this research, the team used the slitting method.

Figure 5 shows a wheel with a sample removed. Strain gages were attached to the sample. A slit was created by electrical discharge machining (EDM) starting from the tread surface and continuing radially to a depth of approximately 2 inches. During the machining, the strain was recorded until the slit was 1.60 inches deep. The pre-existing residual stress was calculated from the measured strain values. Figure 6 shows a sample with a slit.

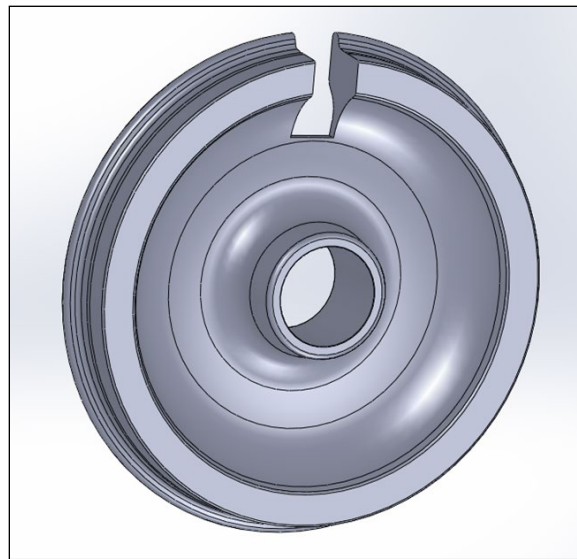


Figure 5. Wheel with Residual Stress Sample Removed

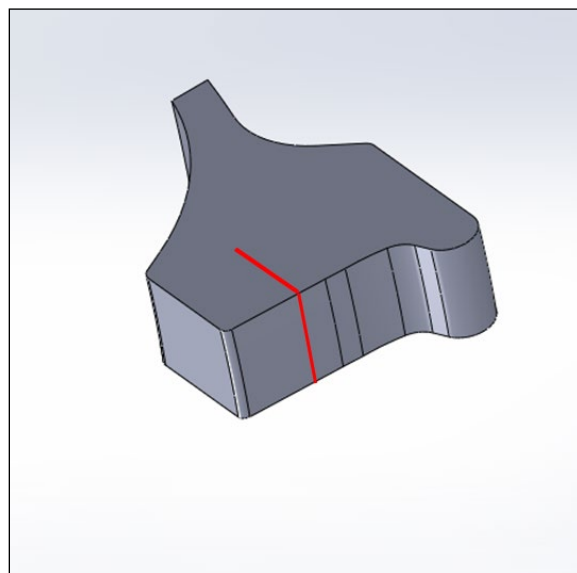


Figure 6. Residual Stress Sample, with EDM Slit Indicated in Red

3.2 Test Method

Researchers purchased four new unmounted as-manufactured wheels from the existing stock of an independent wheel shop. Included in this purchase were four wheels from Manufacturer A and four from Manufacturer B with samples cut from each wheel.

For each sample, the residual stress was calculated at specific depths, up to 1.60 inches. Each cut was made 2.00 inches from the front rim face of the wheel. Negative stress values are compressive and positive values are tensile.

3.3 Results

Figure 7 and Figure 8 show the average axial residual stress from each of the wheels. Figure 7 shows the stresses over the full depth of the cuts, and Figure 8 shows the area near the tread where the VSRs usually initiate. The team made the following observations from these plots:

- There are minor differences between the residual stress patterns that result from the heat treat/quenching operations used by these two manufacturers.
- The samples from Manufacturer A have a lower magnitude compressive axial residual stress near the tread surface (15 ksi to 55 ksi) that remains compressive to at least a 0.30-inch radial depth.
- The samples from Manufacturer B have a more consistent stress pattern with a higher magnitude compressive axial residual stress (45 ksi to 65 ksi) near the tread surface that quickly drops to a value near zero stress around 0.15- to 0.20-inch radial depth, and then reaches a slightly compressive peak again at a depth of about 0.40 inch.
- The samples from Manufacturer A and some samples within the same wheel had initial variations.
- Manufacturer B samples showed less variation near the surface for each of the four wheels and from samples within the same wheel.
- Results from both manufacturers were very similar, within 1 ksi at depths below 1 inch.
- None of the samples exceeded 5 ksi tensile axial residual stress at any of the test depths. This is a positive finding because tensile residual stresses can promote crack growth.
- The tensile axial residual stresses developed during the manufacturing process have much smaller magnitudes compared to the tensile axial residual stresses developed from cold working of the wheels during revenue service.
- The results indicate the residual stresses generated during manufacturing are not likely to be a significant contributor to VSR formation.

Work hardening and increased residual stress occur quickly when the wheel is in service. The FEA performed as part of this research showed that an axial residual compressive stress of at least 43 ksi develops beneath the tread after only five cycles.

Work performed at the Transportation Technology Center (TTC) shows that residual axial tensile stress increases during service, nearly reaching a steady state at around 10,000 miles. The transition from compressive to tensile axial residual stress migrates radially deeper in the wheel during work hardening [5].

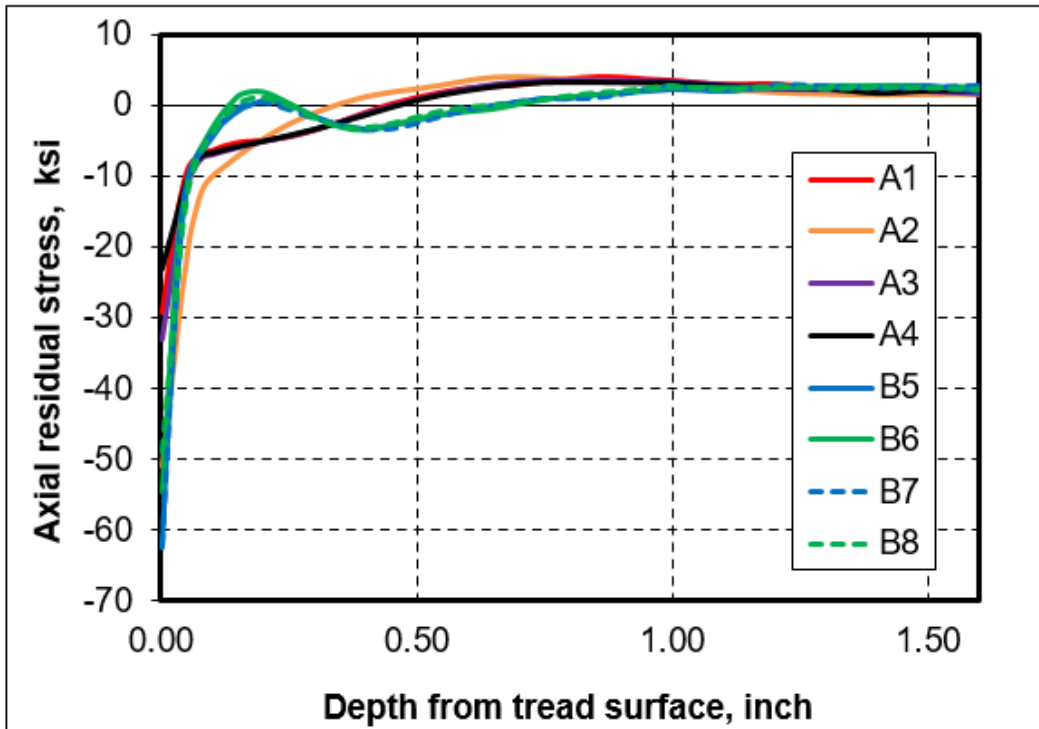


Figure 7. Axial Residual Stress from Tread Surface to Depth of 1.60 inches

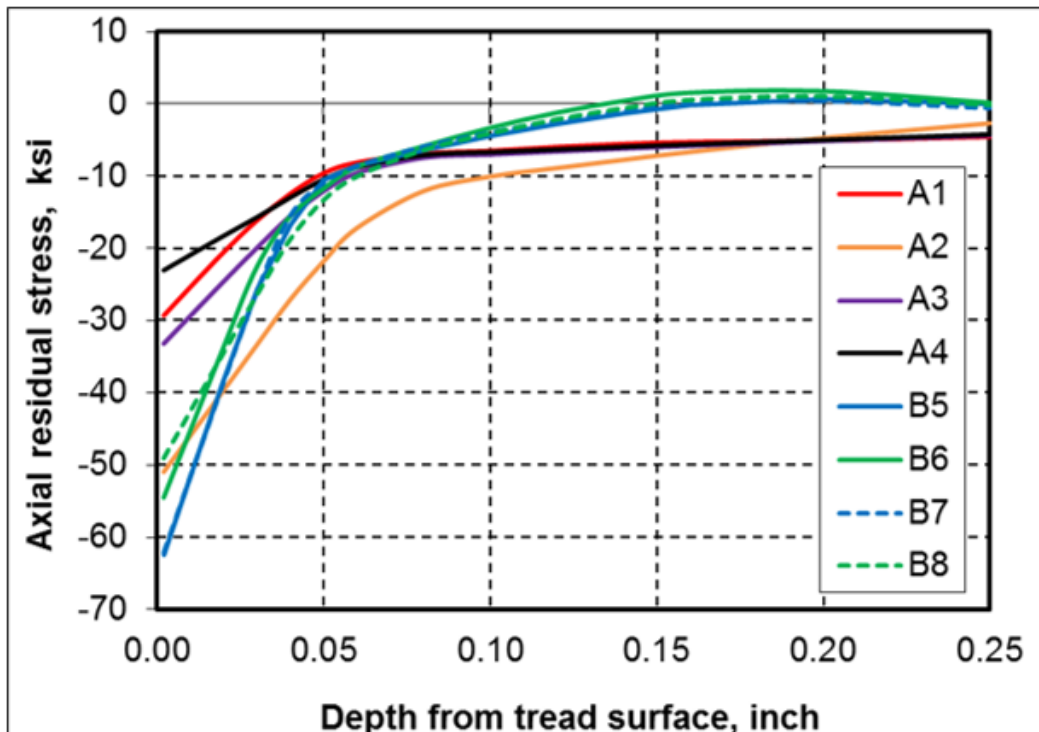


Figure 8. Axial Residual Stress in the Near Surface Region

4. Wheel-Rail Rolling Contact Stress and Fatigue Analysis

4.1 Stress Analysis Method and Parameters

The Center for Railway Research at Texas A&M University performed the FEA in this report. Abaqus 6.9-EF (SIMULIA 2010a) software was used to perform the analyses, which consisted of a railroad wheel rolling along a short section of rail, as shown in [Figure 9](#).

A vertical load of 36 kips, which is essentially equivalent to a gross rail car load of 286,000 pounds, was used for the vertical load in this analysis. Lateral, longitudinal, and thermal loads were not considered in this work [7]. Other parameters used were:

- Friction coefficient of 0.3
- No displacements along longitudinal axis of axle (lateral direction)
- Rail constrained in lateral and longitudinal directions where ties would be located
- Elastic and inelastic material behavior

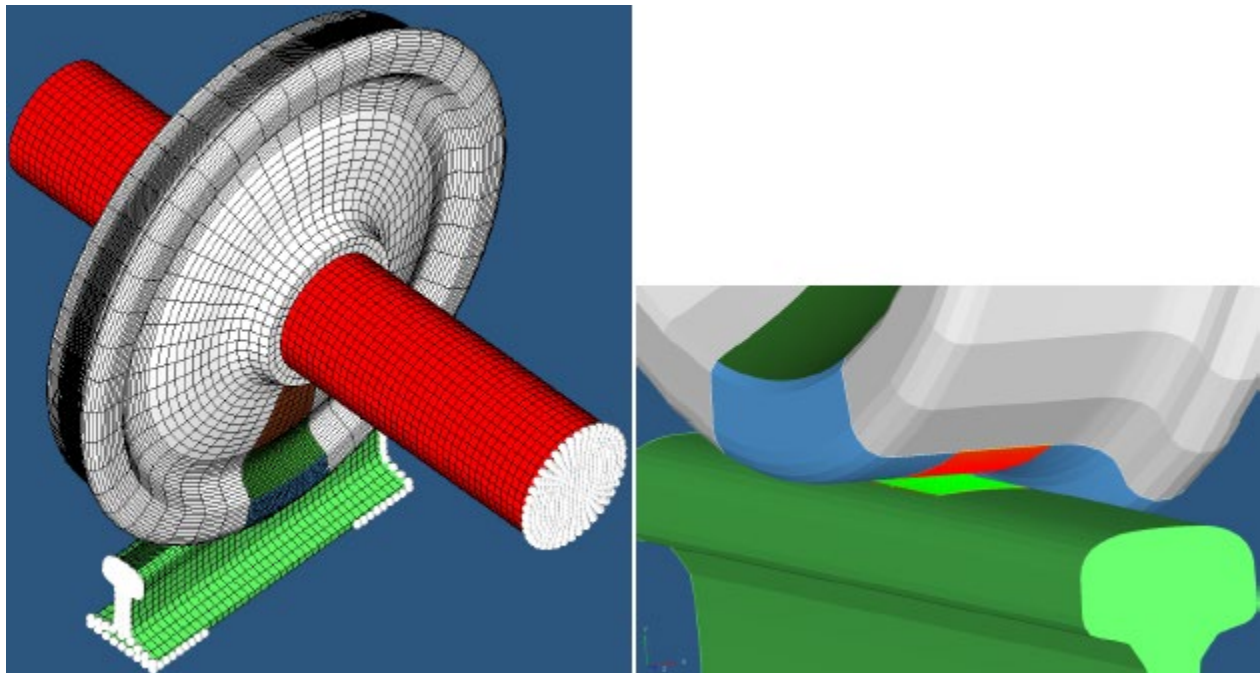


Figure 9. FE Model: (left) Boundary Conditions, (right) Wheel-Rail Contact Interface

For better results, the FE mesh in and near the contact areas was greatly refined, as shown in [Figure 10](#) and [Figure 11](#). The element size in the refined areas is about 0.051 inch wide by 0.055 inch deep by 0.039 inch long in the rail, and about 0.051 inch wide by 0.055 inch deep by 0.079 inch long in the wheel. In total, the FE model is comprised of about 340,000 elements [7]. The rolling simulation was performed by rolling the FE wheel model 2.8 inches in 0.04-inch increments.

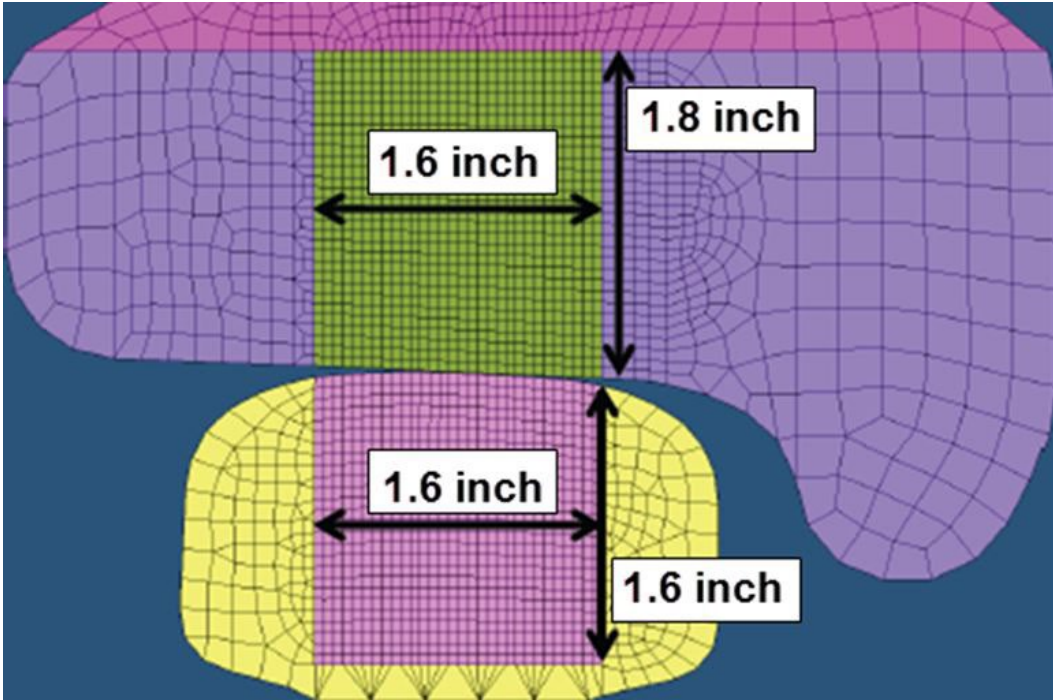


Figure 10. Cross Section of Refined Meshes for Rail and Wheel
Note: 1.6 inch (40 mm) and 1.8 inch (45 mm)

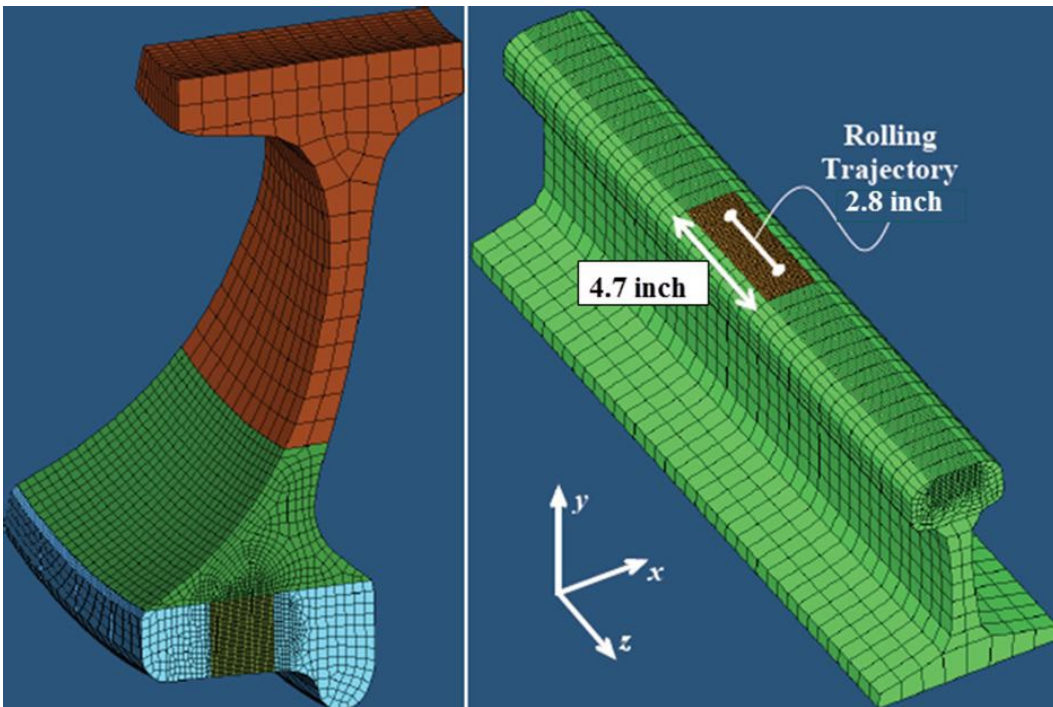


Figure 11. Refined Meshes and Contact Areas for Rail and Wheel
Note: 4.7 inch (120 mm) and 2.8 inch (71 mm)

Figure 12 shows the location of the stress evolution measurements; this node is approximately 0.59 inch below the running surface.

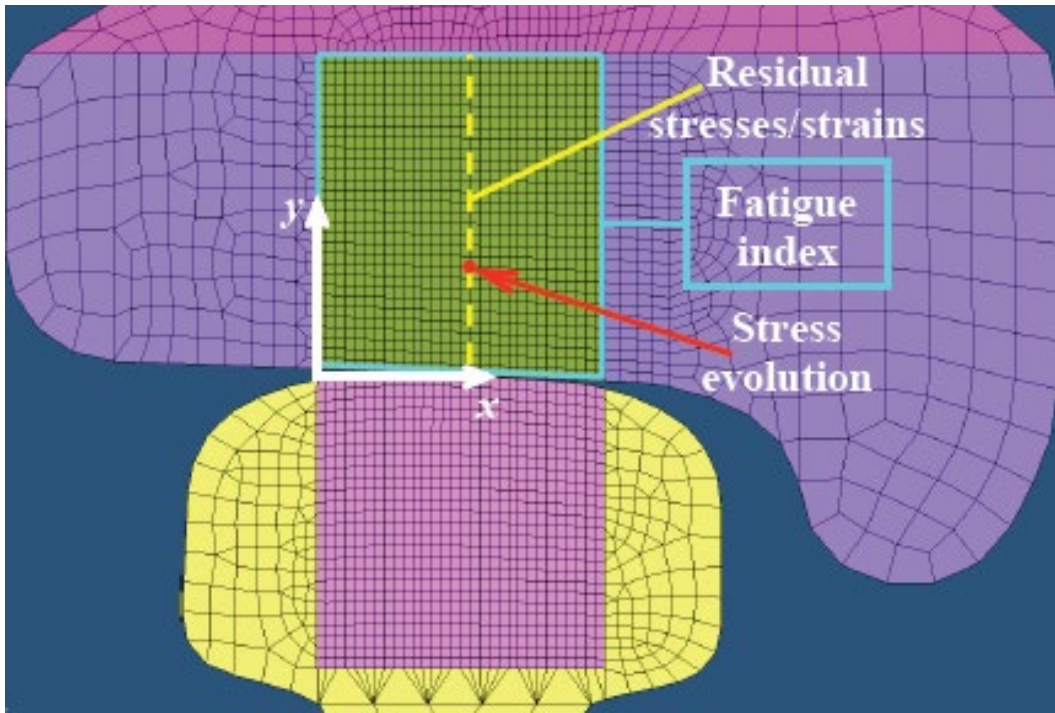


Figure 12. Stress and Fatigue Index Measurement Locations in the Wheel

4.2 Stress Analysis Results

The FE model was rolled over the contact area several times until the stress-strain response of the material had stabilized. This occurred after the fifth cycle (Figure 13) and agrees with findings by Ekberg [7]. In the study under this task order, the stress-strain responses from the sixth loading cycle were used to obtain the fatigue related results.

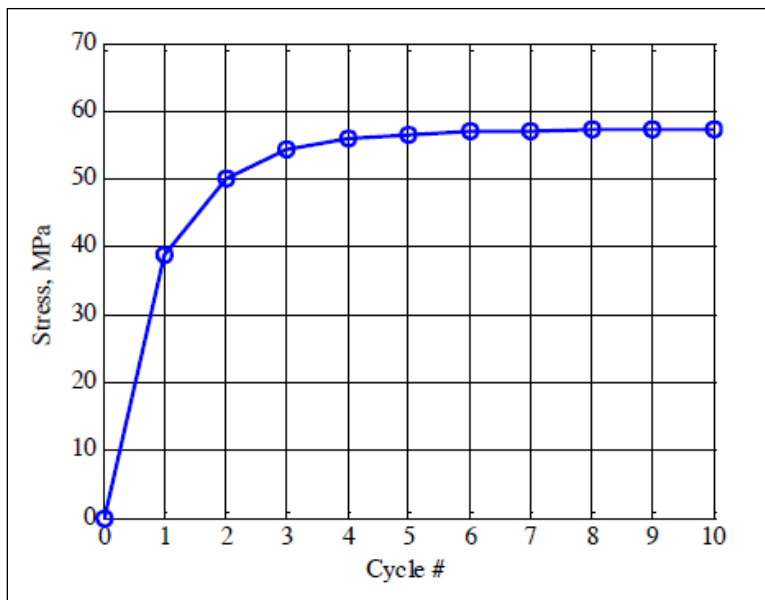


Figure 13. Cyclic Residual Stress Evolution in the Wheel [5]

The residual stress and residual strain plots shown in Figure 14 and Figure 15, respectively, show the distributions after the fifth load cycle. The residual axial tensile stress values (σ_x) agree very well with results reported by Lonsdale et al. [5]. The FE model does not account for residual stresses imparted during the heat treat and quenching operations, and thus shows a tensile axial residual stress at the tread surface and transitions to a compressive state at a radial depth of about 0.039 inch.

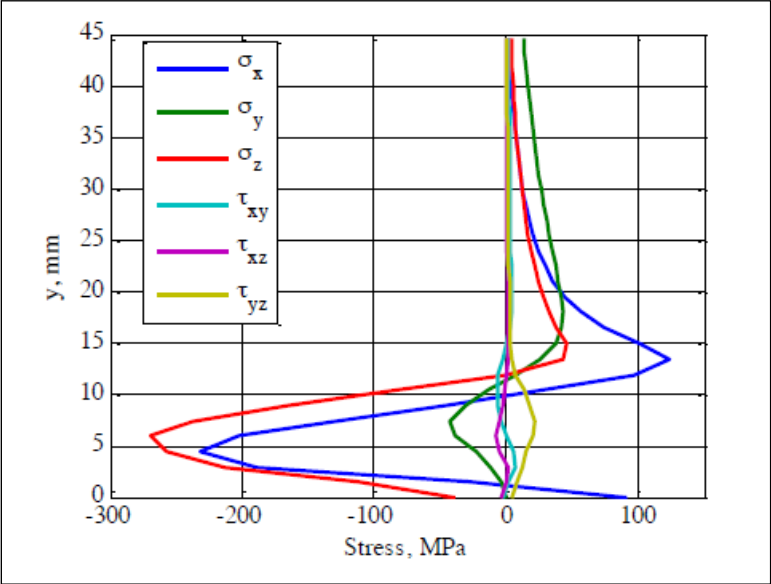


Figure 14. Residual Stress Distribution after the Fifth Load Cycle Along a Line in the Wheel’s Cross Section of Interest [7]

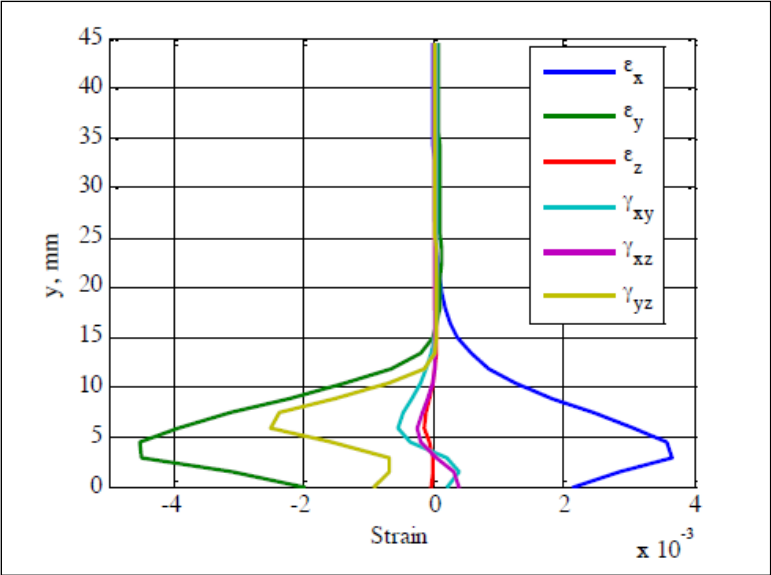


Figure 15. Residual Strain Distribution after the Fifth Load Cycle Along a Line in the Wheel’s Cross Section of Interest [7]

4.3 Findley Fatigue Model Background, Method, and Parameters

The second part of the analysis consisted of a prediction of rolling contact subsurface fatigue using the Critical Plane Findley Fatigue Model. This method is used to predict fatigue crack initiation under multi-axial nonproportional stress conditions [7]. This method assumes that fatigue cracks will initiate along planes where a linear combination of the shear stress amplitude, $\Delta\tau/2$, and a fraction of the normal stress, σ_n , during a load cycle exceeds the ultimate stress of the wheel material, as shown in Equation 1.

$$F = (\Delta\tau/2 + \kappa\sigma_n)_{ultimate} \quad (\text{Equation 1})$$

Failure is supposed to occur at the point and on the plane where F value exceeds the ultimate stress during a rolling cycle. The constant κ is determined experimentally through tests involving two or more stress states. For ductile materials, κ typically ranges from 0.2 to 0.3 [7].

To evaluate the Findley criterion, the stress-strain time history obtained for the FE model's sixth loading cycle was imported into MATLAB for post-processing.

4.4 Findley Fatigue Model Results

The Findley fatigue index was calculated at each node of the FE model in the area of interest to obtain the most accurate fatigue crack initiation life. Then, the search for critical planes was performed by evaluating the Findley fatigue index at every point of interest on a series of planes at various angles [7]. Previous work from Tangtragulwong (2010) found that κ is approximately 0.3 for pearlitic rail steels.

Figure 16, Figure 17, and Figure 18 show the maximum Findley fatigue index at values of $\kappa = 0$, $\kappa = 0.3$, and $\kappa = 1$, respectively. At $\kappa = 0.3$, the maximum Findley fatigue index value was 31.3 ksi at a depth of approximately 0.15 inch in the wheel [7].

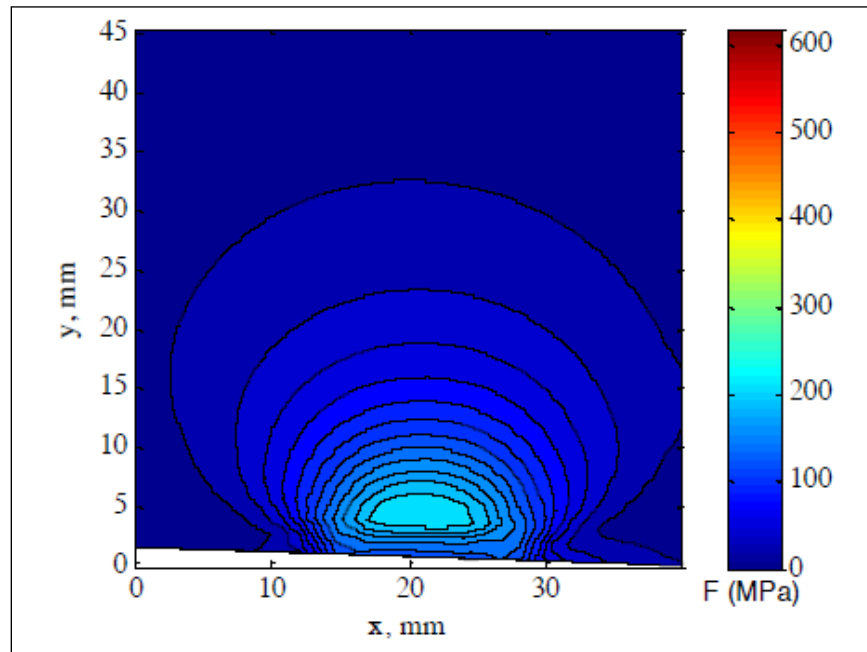


Figure 16. Maximum Findley Fatigue Index for $\kappa = 0$ [7]

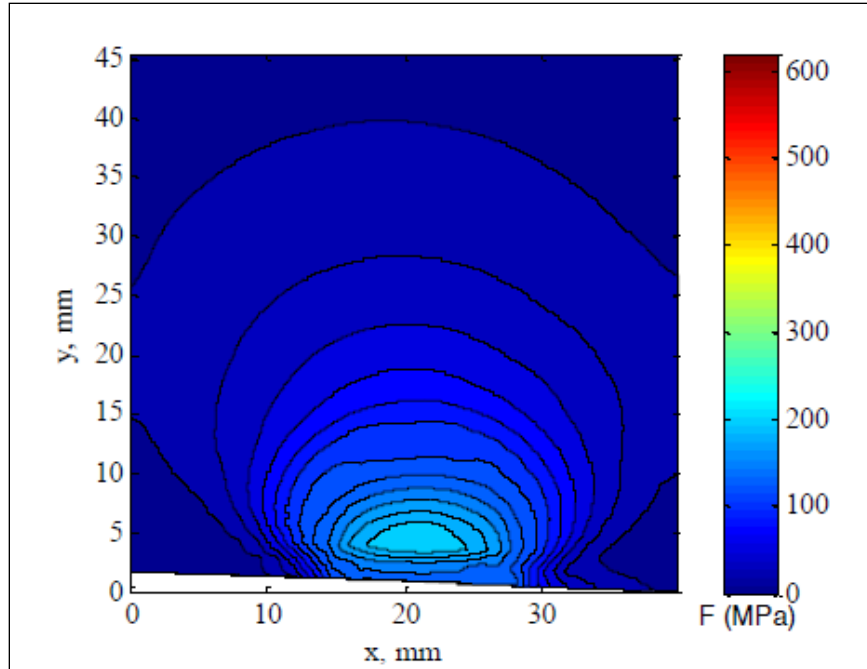


Figure 17. Maximum Findley Fatigue Index for $\kappa = 0.3$ [7]

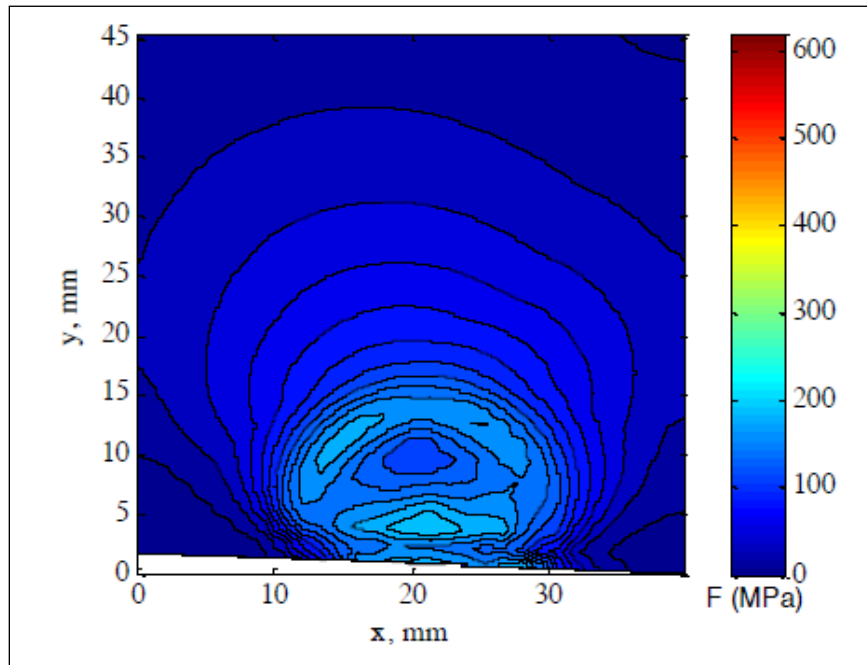


Figure 18. Maximum Findley Fatigue Index for $\kappa = 1$ [7]

4.5 Strain-Based Critical Plane Fatemi-Socie Fatigue Model Background, Method, and Parameters

The Fatemi-Socie Fatigue Model uses a strain-based critical plane criterion to estimate the fatigue crack initiation life of the FE model. As with the Findley criterion, the stress-strain time

history obtained for the FE model's sixth loading cycle was imported into MATLAB where the Fatemi-Socie fatigue criterion was applied.

The physical basis of the Fatemi-Socie Model is that irregular shapes of crack surfaces produce friction forces that oppose shear deformations along the crack's plane (Figure 19). This mechanism limits crack growth, thereby increasing the fatigue life of the material. If tensile stresses normal to the plane of the crack are present, they reduce the normal forces on the crack surfaces, reducing friction forces acting on the crack faces. If this reduction takes place, the crack tips must carry a larger fraction of the shear forces, which is assumed to favor crack growth [7].

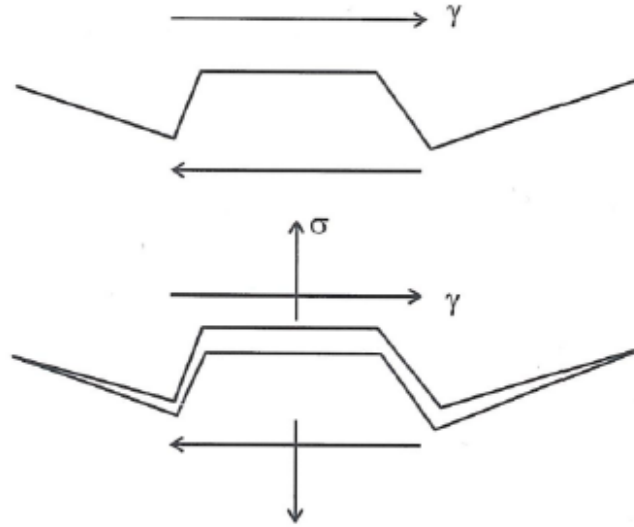


Figure 19. Physical Basis of the Fatemi-Socie Fatigue Model [9]

The Fatemi-Socie Model considers the interaction between cyclic shear strain amplitude and normal stress at a specific point on a particular plane during a load cycle. The normal stress across a plane accounts for the influence of friction. The model is shown in Equation 2:

$$FS = \left[\frac{\Delta\gamma}{2} \left(1 + \eta \frac{\sigma_n}{\sigma_y} \right) \right]_{\max} \quad (\text{Equation 2})$$

where $\Delta\gamma$ is the difference between the maximum and minimum shear strains in a cycle, σ_n is the maximum normal stress in a cycle, σ_y is the yield stress of the material, and η is a material constant, which accounts for the sensitivity of the material's fatigue resistance to normal stresses [7].

4.6 Strain-Based Critical Plane Fatemi-Socie Fatigue Model Results

The Fatemi-Socie fatigue index was calculated at each node of the FE model in the area of interest (see Figure 12). As with the Findley fatigue index, the Fatemi-Socie was evaluated at every point of interest on a series of planes at various angles [7]. Previous work from Tangtragulwong (2010) found that a value of $\eta = 1$ correlated best for pearlitic rail steels.

Figure 20 through Figure 23 show the maximum Fatemi-Socie fatigue index at values of $\eta = 0$, $\eta = 1$, $\eta = 3$, and $\eta = 1$, respectively. At $\eta = 1$, the maximum Fatemi-Socie fatigue index value was 0.19 psi at a depth of approximately 0.15 inch in the wheel [7].

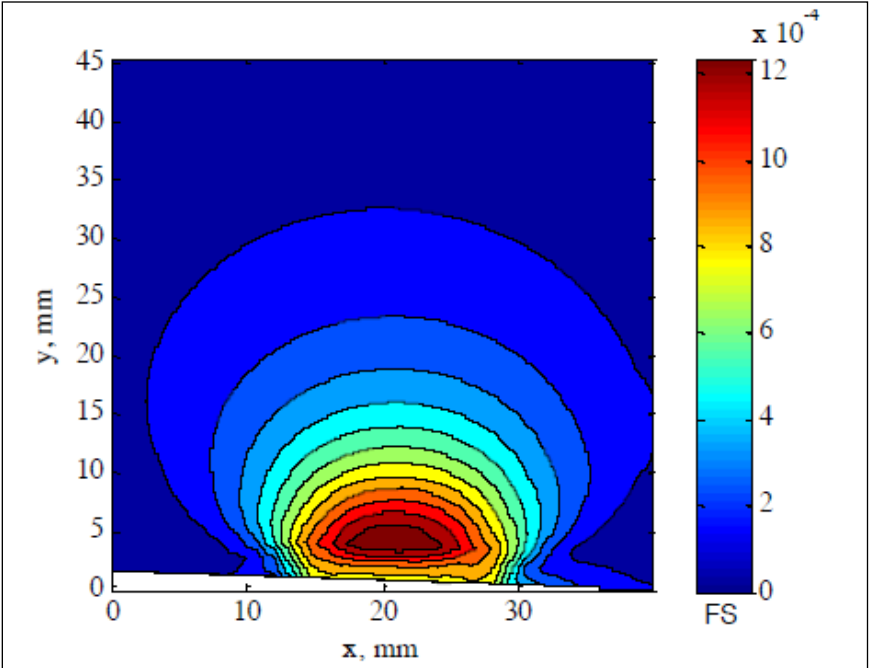


Figure 20. Maximum Fatemi-Socie Fatigue Index for $\eta = 0$

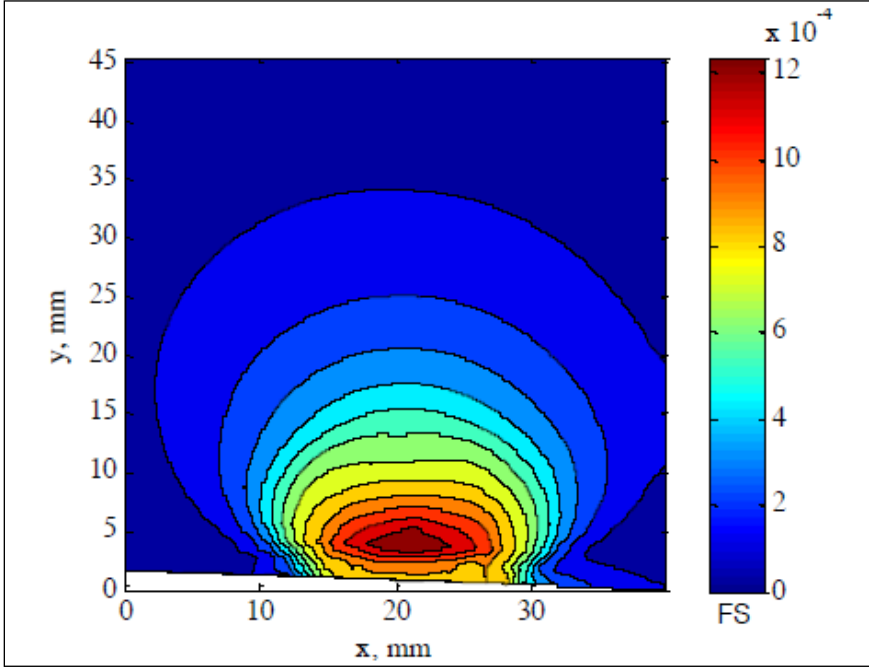


Figure 21. Maximum Fatemi-Socie Fatigue Index for $\eta = 1$

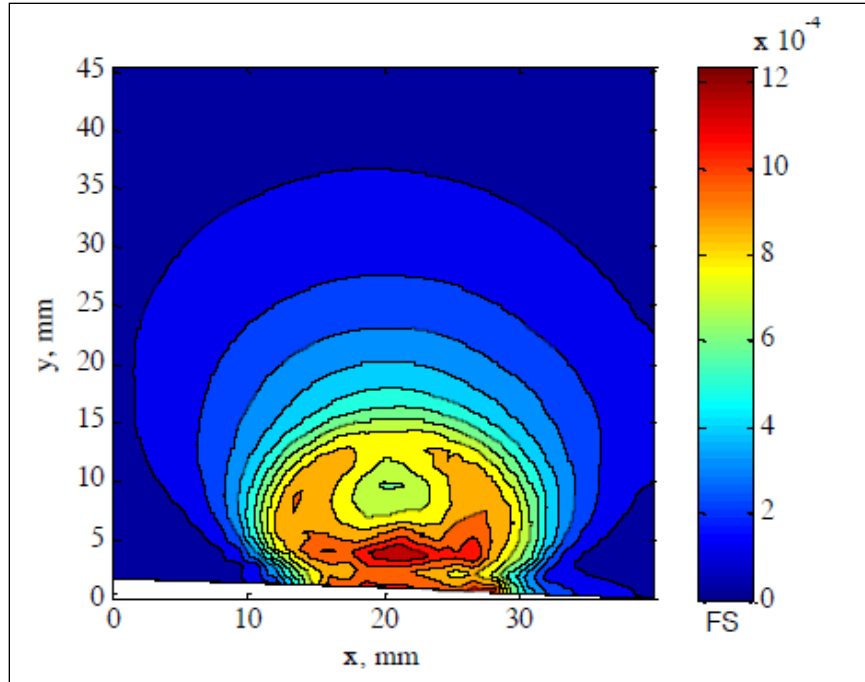


Figure 22. Maximum Fatemi-Socie Fatigue Index for $\eta = 3$

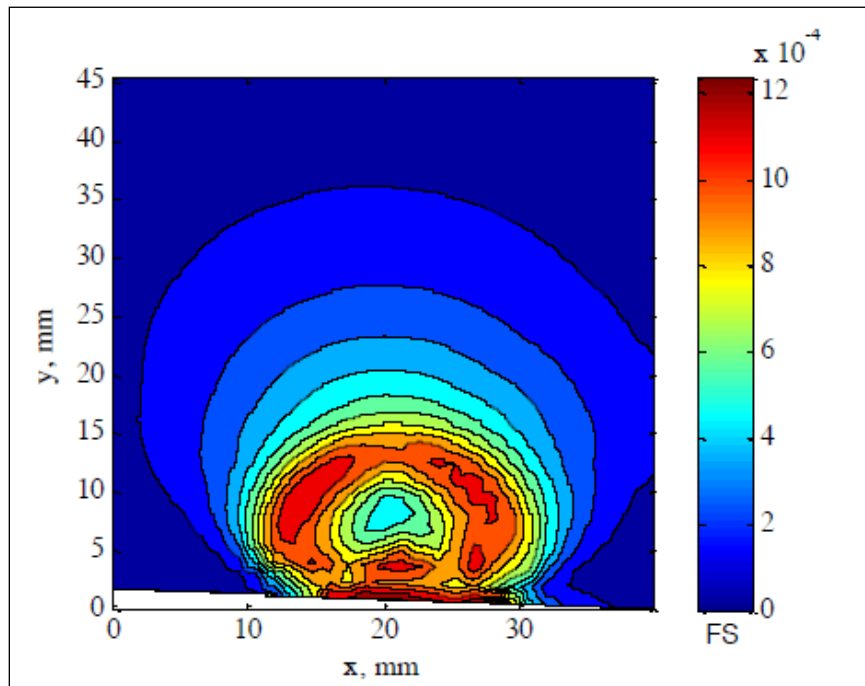


Figure 23. Maximum Fatemi-Socie Fatigue Index for $\eta = 5$

4.7 Stress and Fatigue Analysis Findings

The FEA successfully predicted the evolution of residual stresses in wheels due to the work hardening effects of revenue service rolling contact with the rail. In the analysis, the residual stresses stabilized after five load cycles. While this may seem to be a low number of wheel revolutions to achieve a steady state residual stress, this prediction is for one unique lateral

contact location at the nominal vertical wheel load. Additionally, the measured residual stresses in wheels in service at FAST have been reported to reach values similar to those predicted by the analysis at the lowest mileage tested (i.e., 3,687 miles or approximately 2 million load cycles) and reach near steady-state values by 10,000 miles (i.e., approximately 5.6 million load cycles) [5].

The fatigue lives predicted by both the Findley and Fatemi-Socie indices were very similar, showing about 240,000 cycles and about 220,000 cycles, respectively. These values may also seem low, but they represent the number of load cycles to crack nucleation, not the propagation of a crack to a detectable size. Again, the estimate assumes that every load cycle occurs at precisely the same lateral contact location on the wheel.

Perhaps the most significant finding of the analysis is the agreement of the radial depth of the fatigue initiation spot (3.7 mm or 0.15 inch) in both the Findley and Fatemi-Socie methods. This value corresponds well with the median reported radial depth of VSR crack origins: “Origin radial depths were similar for both VSR and broken flange wheels and ranged from 0.10 inch to 0.25 inch below the tread surface with a median value of 0.17 inch.” [1]

5. Laboratory Creation of a VSR

5.1 Background

Wheel manufacturers and research teams have tried to create VSRs under controlled conditions in the past. A rolling load machine, like that shown in [Figure 24](#), was used on a wheel known to have a large subsurface horizontal crack. An initial vertical load application of 60,000 pounds was periodically increased up to a maximum of 90,000 pounds [1]. This was performed twice; both times the machine failed and no VSR was created. Microscopy of the crack showed a small amount of trans-granular crack propagation. A research team also tried to create a VSR using a drop hammer to simulate impact. A tread damaged wheel was impacted over 31,000 times with a drop hammer, producing loads of 250–300 kips [6]. It resulted in severe deformation of the wheel, but no VSR. The approach for this past research is detailed in [Section 5.2](#).

5.2 Test Method

Researchers developed a test plan to create a VSR using a rolling load machine. The primary goal was to prove that a VSR can be created under controlled conditions in a laboratory. [Figure 24](#) shows the rolling load machine setup at TTC.



Figure 24. Rolling Load Machine at the TTC

In this machine, the wheel remains stationary and the rail reciprocates under it. The load was variable, with a maximum of 50 kips. The test began with a load of 36 kips, which is the approximate load experienced by a wheel under a car with a gross weight of 286,000 pounds. The load was then increased to 50 kips maximum.

To simulate a large VSR crack, a slit was plunge cut in a service worn wheel by using an abrasive disk. The purpose of the slit was to skip the crack formation (i.e., early propagation portion of the VSR failure process) and reproduce the final stage of failure. The maximum depth of the slit was 2.0 inches, and the width was 0.11 inch. [Figure 25](#) shows the geometry of the slit. The slit was cut 2.2 inches from the front rim face of the wheel. The wheel was adjusted laterally in the rolling load machine so that the contact between the wheel and rail was centered near the

crack. Ultrasonic testing was used to verify the crack depth and geometry before testing began. After each day's testing, the wheel was ultrasonically tested to determine whether the crack propagated.

The assumption was that the wheel with the machined slit would produce a VSR-like failure under the rolling load machine. If a VSR occurred, a wheel containing a smaller defect would be tested. With this approach, it was thought that parameters that led to VSRS could be determined.

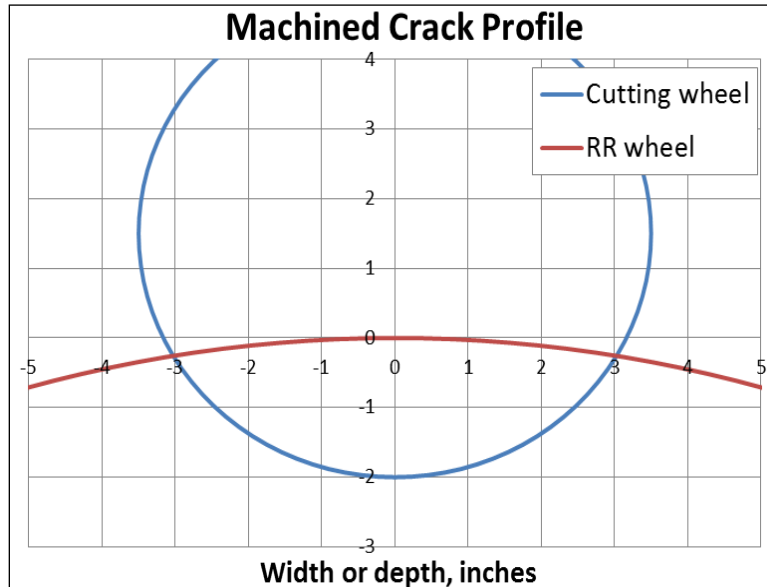


Figure 25. Geometry of Slit in Wheel

5.3 Results

Figure 26 shows the vertical load was increased at certain intervals from 36 kips to the maximum of 50 kips. After a total 1.88 million cycles, no crack propagation was detected ultrasonically. The test was halted after discussions with other research personnel concerning VSR mechanisms, the test setup, visual inspection of wheels, and mechanical property calculations. Metallography was not performed on the crack.

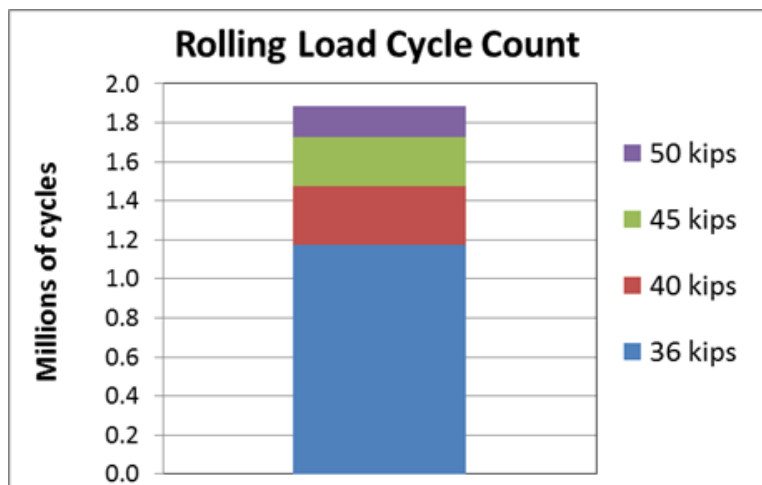


Figure 26. Rolling Load Cycle Count

The following are offered as possible reasons for no crack propagation:

- The machined slit was much wider than a naturally induced crack, and therefore did not produce the same stress intensity that would be expected at the tip of a crack of the same length and depth.
- The loading conditions did not include any impact forces. The revenue service environment includes occasional impacts when a wheel negotiates a frog or a rail joint. Additionally, most VSR wheels have a history of impact load readings from wayside wheel impact load detectors. This impact loading could play a role in the crack propagation.
- An induced slit made with a grinding wheel leaves the material surface of the cut in a different disposition and less likely to propagate than the surface of a naturally made crack due to wheel metallurgy and service conditions.

The exact mechanisms of VSR formation and propagation are still unknown, but new investigative approaches are being explored in other research.

6. Conclusions

The frequency of broken flanges or rims for freight car wheels is higher than that for locomotive wheels, according to data from the FRA Accident Database.

Axial residual stresses in new, as-manufactured wheels from two manufacturers were measured as part of this research. The wheels had compressive residual stresses close to the tread surface, but were near neutral deeper into the wheel rim. The tensile axial residual stresses developed during the manufacturing process have much smaller magnitudes compared to the tensile axial residual stresses developed from cold working of the wheels during revenue service. Large tensile residual stresses can assist in crack propagation, but relatively small tensile residual stresses generated during manufacturing are not likely to be a significant contributor to VSR formation.

The FEA evaluated the evolution of residual stresses and two different fatigue indices in a rolling wheel. The FE model was a three-dimensional model and considered wheel-rail friction and work hardening. The predicted steady-state axial residual tensile stresses agreed well with previously reported values in both magnitude and radial depth.

Both the Findley and Fatemi-Socie methods used in the analyses agreed that the critical radial depth for fatigue initiation in wheels is approximately 0.15 inch, considering both contact stress and residual stress. This value appears to be relevant, because the median radial depth of VSR crack origins from failed wheels has been reported at approximately 0.17 inch.

To better understand the parameters that cause VSRs, a wheel with a slit machined into it was tested on a rolling load machine to cause the crack to propagate. With an initial load of 36 kips, increased at intervals to 50 kips, the test ran for 1.88 million cycles. No crack propagation was detected using ultrasonic methods. The test/research was then terminated to re-evaluate the possible mechanisms of VSR formation.

Possible reasons for the lack of crack propagation were considered, but the exact mechanisms of VSR formation and propagation are still unknown at this time.

7. References

1. Cummings, S., Sura, V., Mahadevan, S., Oliver, J., & Dedmon, S. (August 2010). Modeling the Vertical Split Rim Failure in Wheels. *Technology Digest, TD-10-028*. Association of American Railroads, Transportation Technology Center, Inc., Pueblo, CO.
2. Office of Safety Analysis (July 2014). [Accident Causes Online Database](#). Washington, DC: United States Department of Transportation, Federal Railroad Administration.
3. Association of American Railroads (2014). *Railroad Facts 2013 Edition*. Washington, DC.
4. Class I Annual Report to the Surface Transportation Board for Year Ending December 31, 2013. Schedule 755 (using Form OEEAA-R1).
5. Lonsdale, C., Oliver, J., Maram, R., & Cummings, S. (October 2013). Development of Railroad Wheel Rim Axial Residual Stress in Heavy Axle Load Service (Paper RTDF2013-4716). In *Proceedings of ASME Conference*. American Society of Mechanical Engineers, New York, NY.
6. Lonsdale, C. (November 2012). [Recent Research to Better Understand Wheel Rim Axial Residual Stress and Vertical Split Rim Wheels](#). Presentation. Amsted Rail.
7. Fry, G., Altamira, L., Story, B., & Kiani, M. (2014). Analytical Investigation of Wheel Fatigue. Center for Railway Research, Texas A&M University, College Station, TX.
8. Ekberg, A. (n.d.). [Rolling Contact Fatigue of Railway Wheels – Towards tread life prediction through numerical modelling considering material imperfections, probabilistic loading and operational data](#). PhD thesis, Department of Solid Mechanics, Chalmers University of Technology, Goteborg, Sweden.
9. Socie, D. F., & Marquis, G. B. (2000). *Multiaxial Fatigue*. Society of Automotive Engineers, Warrendale, PA.
10. Tangtragulwong, P. (2010). Optimal Railroad Grinding for Fatigue Mitigation. PhD dissertation, Department of Civil Engineering, Texas A&M University, College Station, TX.

Abbreviations and Acronyms

ACRONYM	DEFINITION
AAR	Association of American Railroads
EDM	Electric Discharge Machining
FAST	Facility for Accelerated Service Testing
FRA	Federal Railroad Administration
FE	Finite Element
FEA	Finite Element Analysis
Kip	Thousand Pounds
TTC	Transportation Technology Center (the site)
TTCI	Transportation Technology Center, Inc. (the company)
VSR	Vertical Split Rim